OIL RECOVERY IN THE TRANSITION ZONE OF CARBONATE RESERVOIRS WITH WETTABILITY CHANGE: HYSTERESIS MODELS OF RELATIVE PERMEABILITY VERSUS EXPERIMENTAL DATA

Franck Nono[1], Henri Bertin[2], Gérald Hamon[3]
University of Bordeaux[1, 2], TOTAL[3]

This paper was prepared for presentation at the International Symposium of the Society of Core Analysts held in Avignon, France, 8-11 September, 2014

ABSTRACT

Due to its moderate permeability and/or very similar oil–water densities, the oil-water transition zone can extend over a large height and therefore contain a sizable amount of STOIIP. In the literature there is very scarce experimental data available for the oil-water system describing a drainage-imbibition process in the transition zone and practically none of them takes into account the variation of wettability on relative permeabilities. Most of the hysteresis models are based on simple extrapolations and do not incorporate wettability changes along the transition zone which is a key point especially in carbonate reservoirs.

In a previous study [1] we performed steady-state core floods experiments with crude oil/brine on limestone cores over a large range of initial oil saturations and observed that wettability varies with height above the oil-water contact and has a strong impact on both oil and water imbibition relative permeabilities. Moreover we showed that there is no unique relationship between initial and residual oil saturations while the most used hysteresis models ([2], [3], [4]) are based on the same Land's residual versus initial oil saturation relationship.

The most sophisticated models incorporating wettability, such as Skjaeveland's relative permeability hysteresis model [4] show better predictions but still need a lot of inputs that are not always available at laboratory scale.

In this study, we compare our experimental data with the most used hysteresis models of relative permeability and we estimate the uncertainties on predicting oil recovery. We also present a new Kr hysteresis model, using the bounding Kr (relative permeability) curves and incorporating wettability change, which best fits our experimental data.

INTRODUCTION

The oil-water transition zone is the part of the reservoir located between the free water level (FWL) and the dry oil limit [5] where water saturation reaches a near constant and irreducible value. In this zone, capillary pressure and thus saturation vary with height above the oil water contact, so as wettability ([1], [6]). The downstructure of the transition zone may exhibit water-wet behavior whereas the upstructure may have mixed-wet or oil-wet characteristics ([6], [7]). While primary drainage controls the primary water distribution in transition zone, oil recovery by waterflooding in the transition zone will be characterized by imbibition process. Wettability and pore structure may have an important influence on the oil recovery ([1]), specifically on the oil and water relative permeabilities.

We recently investigated drainage-imbibition processes using crude oil/brine system, in the transition zone of two different limestones. The scanning imbibition Kr curves were obtained after an ageing time at increasing initial oil saturations (primary drainage) to alter wettability. The two limestones (Richemont and Estaillade) exhibited different pore size distributions: unimodal and bimodal pore size distributions, but had almost the same mineralogy. According to the experimental data (figures 1 to 6), the following suggestions were made:

- Wettability has an influence on both water and oil relative permeabilities.
- Wettability varies with height above the oil water contact.
- The trapping sequence depends on wettability and pore structure.

Therefore, deriving scanning imbibition Kr curves identical to the bounding imbibition Kr, curve i.e. at the highest initial oil saturation, seems to be incorrect. The experimental data showed a change on scanning K_{row} curvatures, which is more pronounced when S_{oi} increases. We observed the same behavior on the scanning K_{rw} curves. For low initial oil saturations, there is practically no hysteresis on scanning K_{rw} and no change in scanning K_{row} curvatures, however a significant hysteresis in K_{rw} curve was observed beyond a critical initial oil saturation.

EXPERIMENTAL DATA vs HYSTERESIS MODELS

We compared our experimental data with the predictions of Killough's, Carlson's and Skjaeveland's relative permeability hysteresis models. For the unimodal limestone (Richemont), the whole experimental data is obtained at oil field normal range of capillary number (10^{-7}).

The Estaillade limestone exhibited a double plateau of capillary pressure, which is in line with a bimodal pore size distribution. By using an oil field normal range of capillary number (10^{-7}), the Imbibition scanning Kr curves departures correspond to initial oil saturations in the lower range of drainage capillary pressure. The maximum oil initial saturation obtained in this case is 0.5 which remains lower than the one obtained with the Richemont (0.78). According to the experimental results of S_{orw} as a function of S_{oi} obtained in this range of capillary number, Richemont limestones follow a Land's type correlation while Estaillade limestones exhibit an almost increasing linear trend (figures 1 and 2). For these comparisons, we used the following oil and water viscosities:
Water : $\mathbf{\mu_w = 0.95}$ cP, Oil : $\mathbf{\mu_o = 34}$ **cP**.

KILLOUGH'S MODEL [2]

A detailed explanation of the Killough's hysteresis approach of deriving the scanning curves can be found in [2]. For the residual oil saturations predictions, the author uses a Land's type correlation with a scaling parameter C obtained on the experimental imbibition bounding curve. It is written as:

$$C = \frac{1}{S_{or,\max}} - \frac{1}{S_{oi,\max}} \quad \textbf{(1)}$$

Where $S_{or,\max}$ is the experimental residual oil saturation obtained on the bounding imbibition curve starting at the highest initial oil saturation $S_{oi,\max}$. C is then used to derive residual oil saturations as a function of initial oil saturations according to equation 1.

The scanning curves (K_{rw} and K_{row}) keep the same curvatures as the bounding experimental imbibition curves at the highest initial oil saturation. This implies a uniform wettability within the transition zone. Likely due to a lack of information in the literature on the end-points K_{rw} variations, the author assumed an increasing extrapolation (linear for most of the time in simulators) towards the primary drainage end-point (K_{rw} = 1 at S_w = 1.).

K_{row} comparisons (figures 7 and 8)

Two different observations can be made: there is a good agreement between the Killough's K_{row} scanning curves and the experimental results for the Richemont limestone (figure 7) and poor agreement for the Estaillade (figure 8). There is an increasing discrepancy between model and experimental results as the initial oil saturation decreases. Killough's approach systematically underestimates the K_{row} values thus oil mobility in the transition zone. The two main reasons are the residual oil saturation evolution and wettability change which are not well predicted.

Wettability tests performed on these two limestones have shown different responses to wettability alteration with crude oil. At high initial oil saturation (at S_{oi} = 0.78), the Richemont limestone exhibits a mixed wet behavior while the Estaillade limestone is practically oil-wet (at S_{oi} = 0.62). This could explain the fact that the Killough's model fits better the Richemont's K_{row} data (smaller change in wettability) than the Estaillade's data (large wettability alteration).

In the same way, Killough's model fits much better the Richemont's residual oil versus initial oil saturation than the Estaillade data. We observed a Land's type correlation for the Richemont data, and an increasing linear trend for Estaillade.

K_{rw} comparisons (figures 9 and 10)

Killough stated that the scanning curves derived with his model always lie between the bounding curves. This statement is not correct considering there is no design constraint in his approach regarding this statement. This is why Killough's model may result in scanning curves which are located outside of the bounding envelopes (figure 9 for Richemont limestone).

Killough's model gives very poor results for both Richemont and Estaillade and overestimates K_{rw}. It's mainly due to the increasing extrapolation of K_{rw} at S_{orw} (purple arrows in figures 9 and 10) which is most of the time used to predict end-points K_{rw} values ([2], [8]).

Fractional flow (figures 11 and 12):
We limited the results to initial oil saturations for which oil mobility is greater than water mobility ($fw(S_{oi}) \leq 0.5$).
On figure 11, the experimental fractional flow curves are very well captured by the Killough's model for the Richemont limestone, but not for Estaillade (figure 12), where there is an increasing gap with the experimental data as the initial oil saturation decreases.

CARLSON'S MODEL [3]

The Carlson's Kr hysteresis model concerns only K_{row}. No hysteresis is assumed in K_{rw}. The scanning K_{row} are drawn parallel to the bounding imbibition K_{row} curve, at the highest initial oil saturation.
Similarly to Killough's model, the scanning curves keep the same shape as the bounding imbibition curve.

K_{row} comparisons (figures 13 and 14)
Unlike Killough's model, Carlson's Kr model shows surprisingly good agreements with the Estaillade data (figure 14) and poor predictions for Richemont (figure 13). This is mainly due to the weakness in predicting residual oil evolution. Estaillade limestone residual oil saturations exhibit an increasing linear trend versus the initial ones. Deriving parallel curves using our bounding imbibition K_{row} curve leads to generate a practically linear trend between the residual oil saturations.

Very poor predictions are observed for Richemont. We also observe an artefact (red circle on figure 13) of the Carlson's model, which depends on the primary drainage and bounding imbibition shapes. The scanning curves could then be out of normal range (negative S_{orw}). It occurs (as it is the case for Richemont) when the difference between the scanning S_{oi} and the imbibition bounding curve oil saturation at the same K_{row} value on primary drainage is higher than S_{orw} (residual oil saturation of the scanning K_{row}).

Fractional flow (figures 15 and 16):
In both limestones, Carlson's model shows optimistic results. Carlson's predictions would generate a shock front saturation, which is not put in evidence by experimental fractional flow curves.

SKJAEVELAND'S MODEL [4]

Skjaeveland's hysteresis Kr model is based on a weighting scheme (equation 2) between oil-wet ($k_{r,oil-wet}^{im}$) and water-wet ($k_{r,water-wet}^{im}$) Kr curves to draw the scanning curves. The imbibition scanning Kr are written as:

$$k_r^{im}(S_o) = \left(\frac{c_{wi}}{c_{wi} - c_{oi}}\right) * k_{r,water-wet}^{im}(S_o) + \left(\frac{c_{wo}}{c_{wi} - c_{oi}}\right) * k_{r,oil-wet}^{im}(S_o) \qquad \textbf{(2)}$$

Where c_{wi} (positive value) and c_{oi} (negative value) are the weighting coefficients which are functions of oil saturation. It takes into account the wettability change within the transition zone. It is assumed that the weighting average (equation 3) might describe any intermediate wet situation.

$$Average-weighting = \left(\frac{c_{wi}+c_{oi}}{c_{wi}-c_{oi}}\right) \quad \textbf{(3)}$$

Using this model means to be in possession of the bounding Kr curves at strongly water-wet and strongly oil-wet conditions, which is rarely the case. As we couldn't perform Kr measurements at oil-wet conditions and predict the variation of water end-points imbibition K_{rw}, we fitted by least squares error method our experimental imbibition scanning K_{row} (figures 17 and 18) and we compared the Skjaeveland's coefficients weighting average evolution obtained versus S_{oi} with the experimental measurements of wettability indices. There is a good consistency with the experimental wettability measurements (figures 19 and 20). This supports the idea of including a wettability parameter in hysteresis Kr models.

NEW HYSTERESIS MODEL PROPOSAL

The new hysteresis model of Kr needs:

- Imbibition Kr curves at the highest initial oil saturation which is representative from the reservoir wettability.
- Primary drainage Kr curves
- Value of S_{orw} at the highest S_{oi}
- A scaling parameter which is a critical oil saturation value

S_{orw} vs S_{oi}

We use an Aissaoui's type Correlation [9] of S_{orw} vs S_{oi} with a piecewise linear relationship. Several experimental measurements of residual versus initial saturations data of the literature ([1], [10]) agree fairly well with Aissaoui's correlation:

1. The lowest range of initial oil saturation is described by: $S_{orw}=0.5 \times S_{oi}$
2. The plateau corresponds to the highest range of initial oil saturations where S_{orw} does not change as a function of S_{oi} and is equal to the experimental S_{orw} achieved at the highest S_{oi} (figure 21). If the residual oil saturation $S_{or,\ max}$ obtained by $S_{oi,\ max}$ is above the half oil recovery trend, there is therefore no plateau, and we keep the increasing linear evolution.

K_{rw} scanning curves

We used a method similar to Killough's approach [2]. The main difference hinges on the constraints to keep the scanning curves to stay within the bounding curves. Instead of direct ratios of relative permeabilities values, we use ratios of the differences between the scanning imbibition K_{rw} curves and the primary drainage one for the same saturation. Using the same saturation normalization as Killough [2], the scanning K_{rw} curves are written as:

$$k_{rw}^{im}(S_o) = k_{rw}^{dr}(S_o) + \left[\frac{k_{rw}^{im,\exp}(S_o^{norm}) - k_{rw}^{dr}(S_o^{norm})}{k_{rw}^{im,\exp}(S_{orw}^{\max}) - k_{rw}^{dr}(S_{orw}^{\max})}\right] * \left[k_{rw}^{im}(S_{orw}) - k_{rw}^{dr}(S_{orw})\right] \quad \textbf{(4)}$$

Where $k_{rw}^{dr}(S_o)$ is the primary drainage K_{rw} value at S_o, $k_{rw}^{im,\exp}$ correspond to the bounding imbibition K_{rw}. As in Killough's model, the hysteresis on K_{rw} values will be scaled according to the end-points imbibition K_{rw} values ($k_{rw}^{im}(S_{orw})$). For low initial oil saturations, $k_{rw}^{im}(S_{orw})$ is found on the primary drainage curve (no hysteresis). According to figures 23 and 24, we had similar observations for both outcrop limestones end-points K_{rw} behavior. In these figures, we plotted experimental end-points K_{rw} ratios which correspond to the ratios between the experimental scanning imbibition end-point K_{rw} (intermediate wettability), with the primary drainage K_{rw} value at the same residual oil saturation. It is written as:

$$\text{end}-\text{point} \quad ratio = r = \left[\frac{k_{rw}^{im,\exp}(S_{orw})}{k_{rw}^{dr,\exp}(S_{orw})}\right] \qquad \textbf{(5)}$$

Where $k_{rw}^{im,\exp}(S_{orw})$ is the end-point scanning K_{rw} value (intermediate wettability) and $k_{rw}^{dr,\exp}(S_{orw})$ corresponds to the primary drainage K_{rw} value at the same residual oil saturation. For water-wet conditions, there is almost no hysteresis on K_{rw} and this ratio is set to be equal to 1 as it is almost the case (experimentally observed) for both limestones for low initial oil saturations (figures 23 and 24). We observed that beyond a critical initial oil saturation, the end-points K_{rw} ratios start to increase exponentially. We then propose to use a scaling parameter which is the critical initial oil saturation. In our experiments, we found this initial oil saturation ($S_{oi,\ critical}$) to correspond to a capillary pressure of almost 0.12 bars for both limestones, or to be almost equal to 65% of the maximum mobile oil saturation obtained (on bounding imbibition curve). Therefore, this term can be adjustable. After scaling the critical initial oil saturation, we can predict the end-point ratios (r function of initial oil saturation) thus the end-points scanning K_{rw} values by using an exponential trend written as:

$$\text{r}(\text{S}_{\text{oi}}) = \text{end}-\text{point} \quad ratio = A * e^{B * S_{oi}} \qquad \textbf{(6)}$$

A and B are scalar coefficients which can be easily calculated with $r(S_{oi,\ critical}) = 1$, and $r(S_{oi\ max})$ is known.

There are fairly good agreements with the experimental data (figures 25 and 26). The hysteresis is well followed. This allows the prediction to fit as well the oil/water ratio mobility evolution versus height above the oil-water contact, for both outcrop limestones.

K_{row} scanning curves

We used a combination of Killough's and Skjaeveland's approach of construction.

Without any imbibition curves at water-wet conditions, we use Killough's method to derive water-wet imbibition curves from the primary drainage curve, starting at the initial oil saturation of the scanning curve. Next, we use Killough's method to derive the scanning intermediate-wettability at the same initial oil saturation, using as the master curve which is the bounding imbibition at the highest S_{oi} ($S_{oi,max}$). We then use a weighting scheme with saturations gap between the derived water-wet curve and the derived intermediate-wet curve to derive the scanning curve at S_{oi} (figure 22).

Let's call $k_{row,w-wet}^{im}(S_{oi}, S_o)$, the scanning K_{row} curve obtained by Killough's model at S_{oi}, using primary drainage as master curve and $k_{row,\text{int}-wet}^{im}(S_{oi}, S_o)$ the one obtained using the bounding imbibition curve departing from $S_{oi,max}$. The weighting scheme to derive the final scanning imbibition K_{row} curve starting at S_{oi} is written as:

$$K_{row}^{im}(S_{oi}, S_o) = \left(\frac{S_{oi,\max} - S_{oi}}{S_{oi,\max}}\right) * K_{row,w-wet}^{im}(S_{oi}, S_o) * + \left(\frac{S_{oi}}{S_{oi,\max}}\right) * K_{row,\text{int}-wet}^{im}(S_{oi}, S_o) \qquad \textbf{(7)}$$

The curves are in good agreements with the experimental data, compared to the literature hysteresis models (figures 27 and 28). Despite little discrepancies, the change in K_{row} curvatures with height above the oil water contact is well followed.

Because of better predictions of the scannings Krw and Krow, the fractional flows for both limestones are well predicted by the model (figures 29 and 30) compared to the hysteresis models results previously investigated.

CONCLUSIONS AND PERSPECTIVES

This paper presents the comparison between experimental drainage and imbibition relative permeability curves along a transition zone of carbonate rocks with the prediction of the most used relative permeability hysteresis models.

The main conclusions are summarized as follows.
- Killough's and Carlson's models do not account for wettability variation as a function of elevation above the free water level.
- The Killough's model overestimates the scanning imbibition K_{rw} and underestimates K_{row} that leads to exacerbate the water mobility, lower oil mobility and underestimate the oil recovery.
- Using Land's correlation for all experiments data leads to great uncertainties on the residual oil saturations while no unique relationship is experimentally observed.
- We proposed a new hysteresis model, which combines Killough's and Skjaeveland's approaches and agrees satisfactorily with our experimental data. This model includes a calibration parameter for K_{rw} predictions which is a critical oil saturation. We found best fitting values for both limestones to be practically similar regarding the maximum mobile saturation or the capillary pressure values.

An ongoing work is performed to simplify the uses and choices of the critical oil saturation.

ACKNOWLEDGEMENTS

We thank TOTAL for financial support and the permission to publish this paper.

NOMENCLATURE

K_{row}	= Oil relative permeability in oil/water system
K_{rw}	= water relative permeability
k_{row}^{im}	= imbibition oil relative permeability

k_{rw}^{im} = Imbibition water relative permeability
$k_{rw}^{im,\exp}$ = Bounding experimental water imbibition Kr
k_{rw}^{dr} = Bounding water drainage Kr
r = End-points K_{rw} ratio
S_o^{norm} = Normalized oil saturation (Killough [2])
S_{oi} = Initial oil saturation
$S_{oi\ critical}$ = Critical initial oil saturation
$S_{oi\ max}$ = Maximum initial oil saturation achieved (bounding imbibition)
S_{orw} = Residual oil saturation
$S_{orw,max}$ = Residual oil saturation achieved (bounding imbibition)

REFERENCES

1. Nono, F., Bertin, H., Hamon, G.: "An Experimental Investigation of the Oil Recovery in the Transition Zone of Carbonate Reservoirs Taking Into Account Wettability Change," IPTC paper 17640, presented at the IPTC, Doha, Qatar, January 20-22, 2014.
2. Killough, J.E.: "Reservoir Simulation With History-Dependent Saturation Functions"; SPEJ (February 1976) 37; Trans, AIME, 261.
3. Carlson, F. M., 1981: "Simulation of Relative Permeability Hysteresis to the Non-Wetting Phase", Paper SPE 10157 presented at the 56th Annual Fall Technical Conference and Exhibition of the Society of Petroleum Engineers of AIME, San Antonio, TX.
4. Skjaeveland, S.M., Siqveland, L.M., Kjosavik, A., Hammervold, W.L., Virnovsky, G.A.: "Capillary Pressure Correlation For Mixed-Wet Reservoirs", SPE 39497, paper presented at the SPE India Oil and Gas Conference and Exhibition, New Delhi, India, February 17-19, (1998)
5. Ghedan, S.G., Thiebot, B.M., and Boyd, D.A: "Modeling Original Water Saturation in the Transition Zone of a Carbonate Oil Reservoir". SPE Res Eval & Eng. (6): 681-687. SPE-88756-PA, 2006.
6. Hamon, G.: "Field-Wide Variations of Wettability," paper SPE 63144 presented at the 2000 SPE Annual Technical Conference and Exhibition, Dallas, Texas, 1-4 October.
7. Mathew, D. J.; Per, H. V.; Martin, J. B.: "Prediction of Wettability Variation Within an Oil/Water Transition Zone and its Impact on Production", SPE Journal, v.10 (2), p. 185-195, 2005.
8. Kjosavik, A., Ringen, J.K., and Skjaeveland, S.M.: "Relative Permeability Correlation for Mixed-Wet Reservoirs," SPEJ (March 2002) 49–58.
9. Aissaoui A. : ''Étude Théorique et Expérimentale de l'Hystérésis des Pressions Capillaires et des Perméabilités Relatives en vue du Stockage Souterrain de Gaz'', Thèse École des Mines de Paris, 1983.
10. Suzanne, K., Hamon, G., Billiotte, J.: Residual Gas Saturation of Sample Originally at Residual Water Saturation in Heterogeneous Sandstone Reservoirs", SCA2003-14 presented at the SCA 2003 conference, Pau, France (2003).

TABLES AND FIGURES

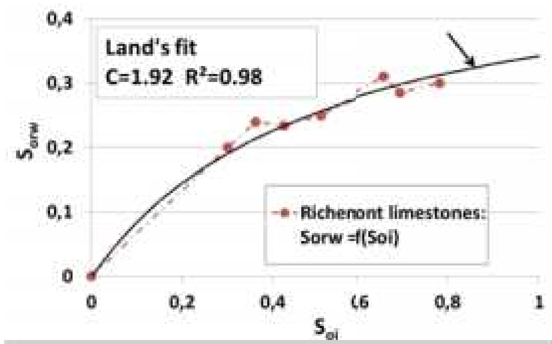

Figure 1: Richemont: Experimental Sorw = f(Soi)

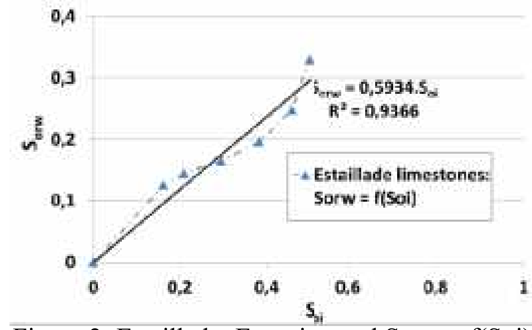

Figure 2: Estaillade: Experimental Sorw = f(Soi)

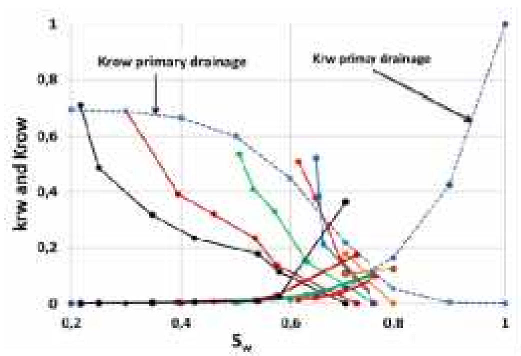

Figure 3: Richemont
Experimental data of Krw and Krow
Oil displaced by water in the transition zone

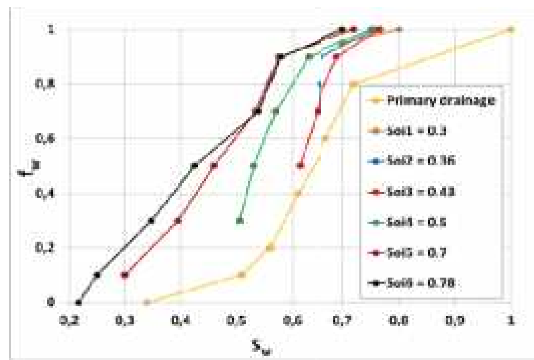

Figure 4: Richemont (**μw = 0.95 cP, μo = 34 cP**)
Experimental results of fw
Oil displaced by water in the transition zone

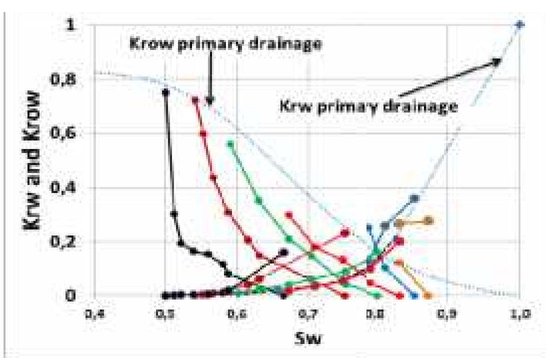

Figure 5: Estaillade
Experimental data of Krow and Krw
Oil displaced by water in the transition zone

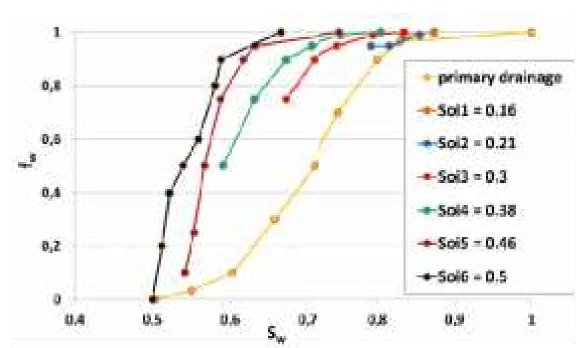

Figure 6: Estaillade (**μ_w = 0.95 cP, μ_o = 34 cP**)
Experimental data of fw
Oil displaced by water in the transition zone

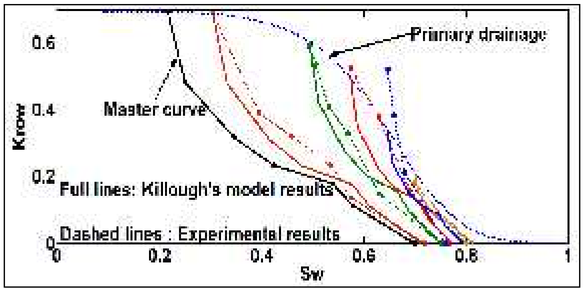

Figure 7: Richemont
Krow Killough’s model results VS experimental data

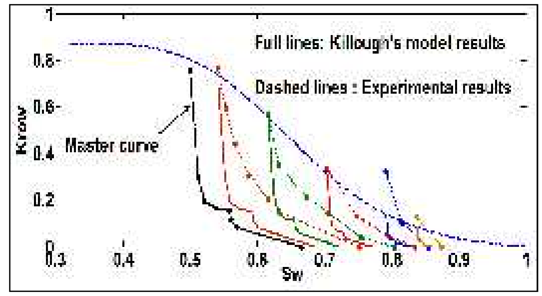

Figure 8: Estaillade
Krow Killough’s model results VS experimental data

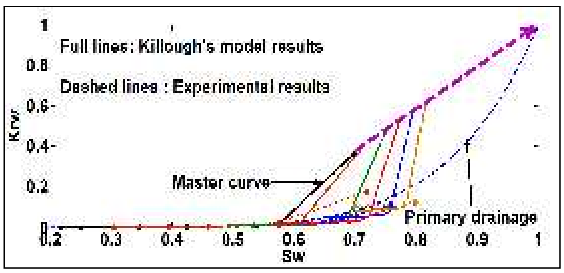

Figure 9: Richemont
Krw Killough's model results VS experimental data

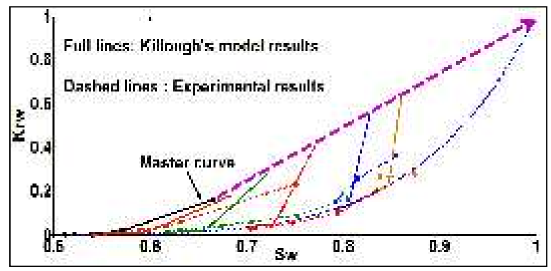

Figure 10: Estaillade
Krw Killough's model results VS experimental data

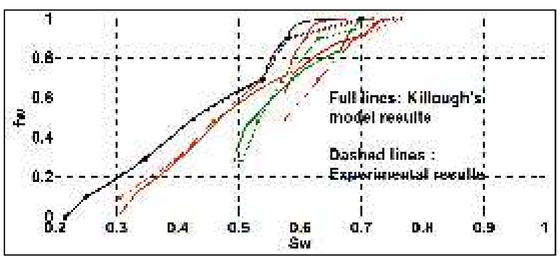

Figure 11: Richemont
fractional flow Killough's model results VS experimental data

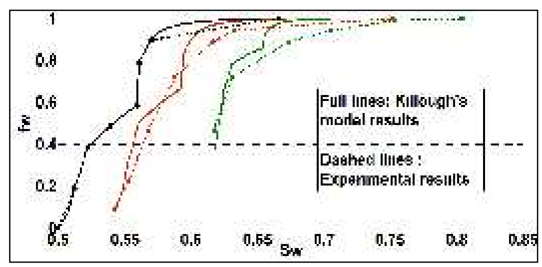

Figure 12: Estaillade
fractional flow
Killough's model results VS experimental data

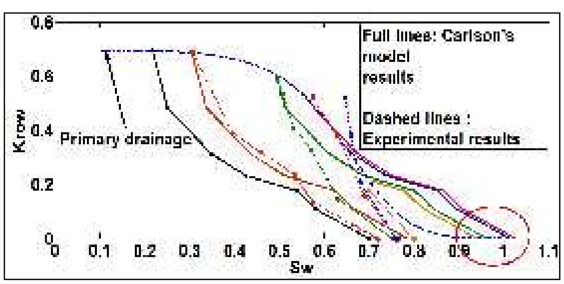

Figure 13: Richemont
Krow Carlson's model results VS experimental data

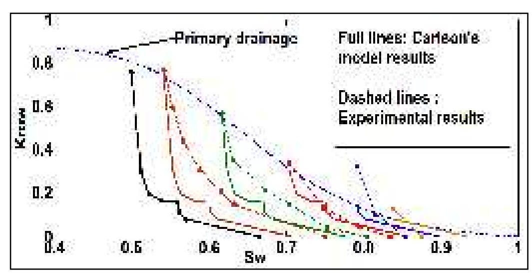

Figure 14: Estaillade
Krow Carlson's model results VS experimental data

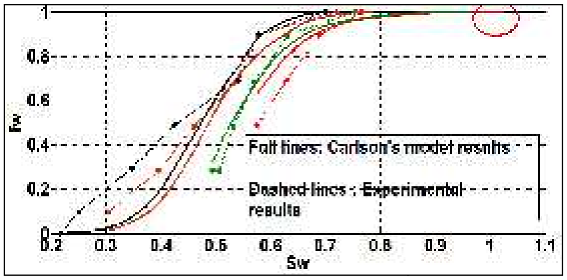

Figure 15: Richemont fractional flow
Carlson's model results VS experimental data

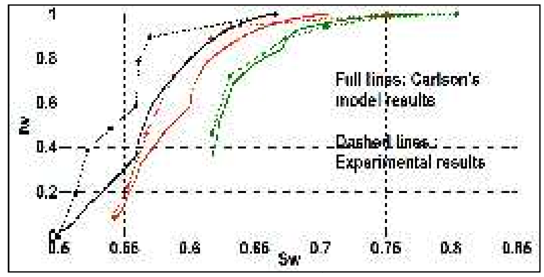

Figure 16: Estaillade fractional flow
Carlson's model results VS experimental data

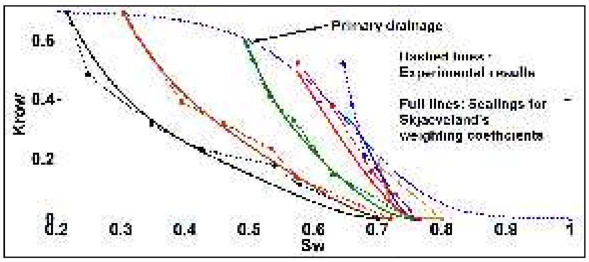

Figure 17: Richemont
Skjaeveland's scaling of experimental Krow

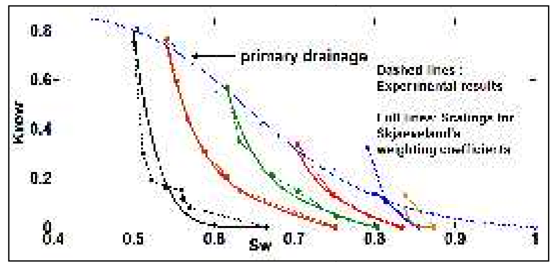

Figure 18: Estaillade
Skjaeveland's scaling of experimental Krow

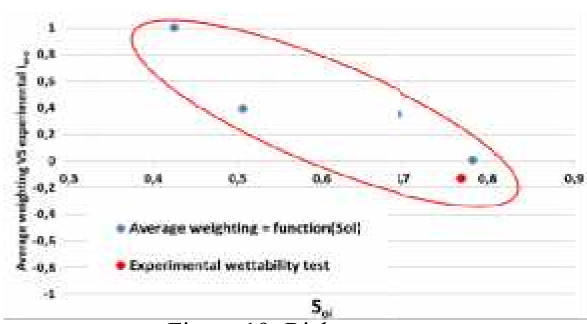

Figure 19: Richemont
Skjaeveland's weighting average versus experimental data of wettability

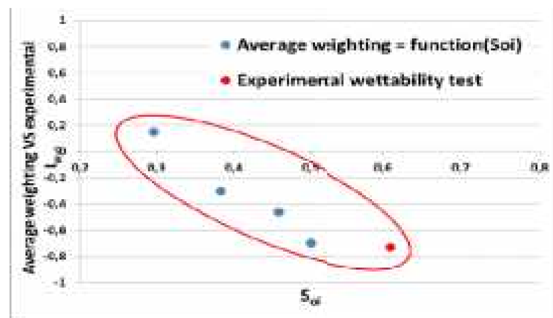

Figure 20: Estaillade
Skjaeveland's weighting average versus experimental data of wettability

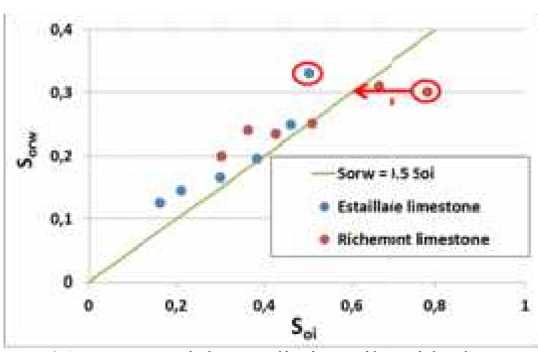

Figure 21: New model - predicting oil residual saturations

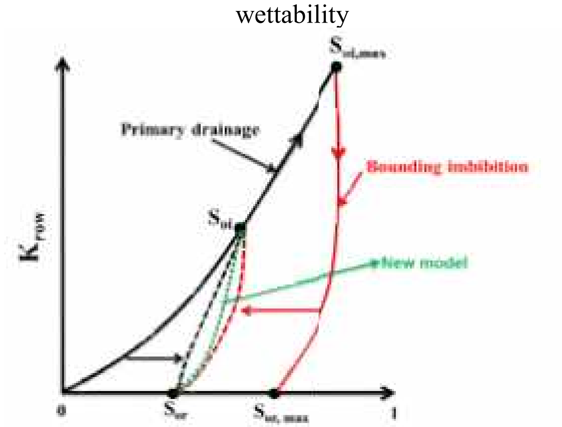

Figure 22: New model - predicting Krow

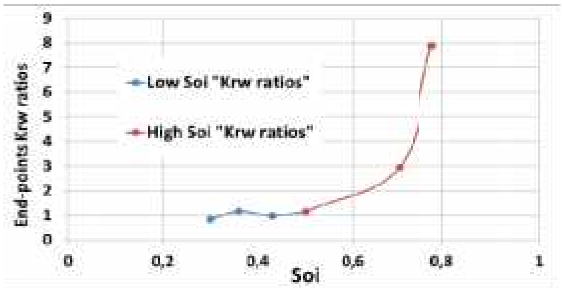

Figure 23: Richemont end-points Krw ratios
(intermediate wettab/water-wet)

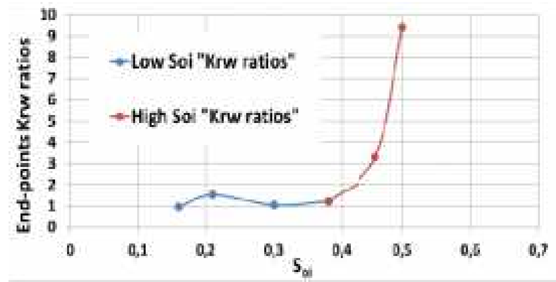

Figure 24: Estaillade end-points Krw ratios
(intermediate wettab/water-wet)

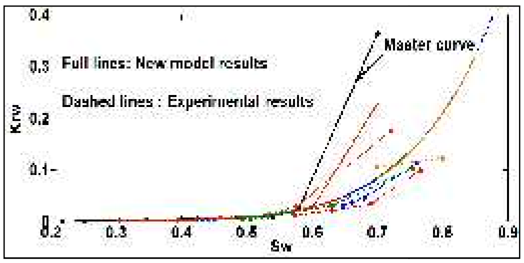

Figure 25: Richemont Krw
New model results VS experimental data

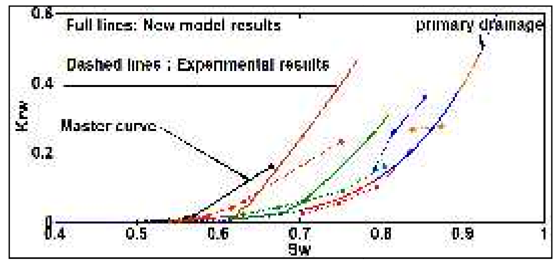

Figure 26: Estaillade Krw
New model results VS experimental data

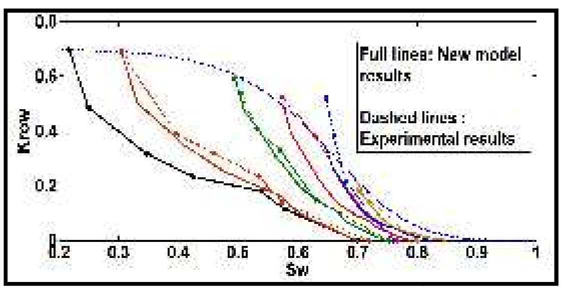

Figure 27: Estaillade Krow
New model results VS experimental data

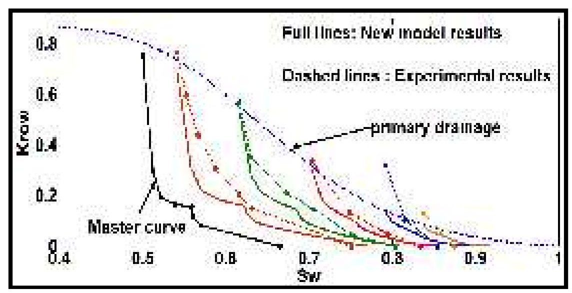

Figure 28: Richemont Krow
New model results VS experimental data

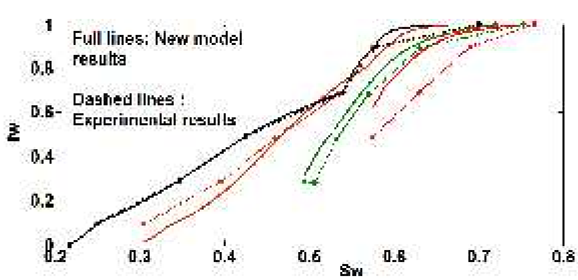

Figure 29: Richemont fw
New model results VS experimental data

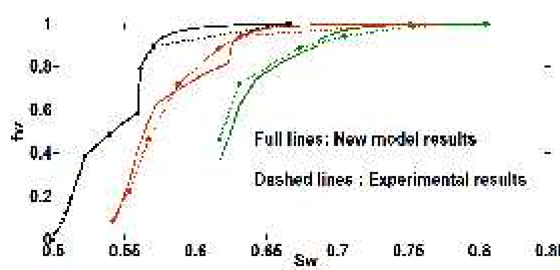

Figure 30: Estaillade fw
New model results VS experimental data